19th Brazilian Congress of Thermal Sciences and Engineering
November 06th-10th, 2022, Bento Gonçalves - RS - Brazil

ENC-2022-0477
VALIDATION OF A CFD CODE WITH LBM APPROACH WITH EXPERIMENTAL DATA FROM A TESLA TURBINE

José Filipe Trilha de Carvalho
Paulo Smith Schneider
UFRGS, Av. Osvaldo Aranha, 99 - Centro Histórico, Porto Alegre - RS, 90035-190
filipecarvalhosw@gmail.com
pss@mecanica.ufrgs.br

Abstract. The study of the Tesla turbine design in the early stages of its development is extremely important for the proposal of new design solutions that provide greater efficiency that increase the field of use of Tesla turbines as a solution for alternative systems of small and medium power generation.
The present work performed simulations via computational fluid dynamics in a three-dimensional, single-phase, and turbulent approach, using the LES turbulence models, in order to evaluate the flow of fluid in the internal region of the Tesla turbine with the stationary rotor. The numerical code based on the Boltzmann lattice method is used as the objective of numerically predicting the torque results, comparing numerical results with experimental data obtained in prototype experiments. Considering the measurement uncertainty associated with 3.45 % to the values of the measured torques, the vast majority of the results presented here contain values within the uncertainty range. Considering that 8.82% of the results obtained with the numerical code presented a variation above 10 % variation in relation to the experimental results, it is considered the code presented a coherent physical behavior, not being necessary adjustments in its parameters for subsequent studies of turbine evaluation with different discs topologies.

Keywords: *Tesla, turbine, CFD, design, discs, topology.*

1. INTRODUCTION

Tesla turbines have been of interest to many researchers in recent times, since it is a form of energy generation that can use renewable fluids. Moreover, it provides benefits such as low design costs, compact size, easy installation and minimized operation, noise and vibrations, as well reduced operating, and maintenance costs. (Batista, 2009).

Regarding the principle of operation of the Tesla turbine, in a very simplified way, the turbine is fed through a converging nozzle that introduces the fluid to the system tangentially entering the discs, which generates the torque on the shaft. The fluid performs a spiral-shaped movement, remaining adhered to the walls until it reaches the slots, these, in the form of a circular oblong positioned near the central axis coupled to the discs, being then conducted to the discharge section of the turbine.

Therefore, the torque generated by the friction of the fluid with the discs can be used in several applications, both for the generation of energy with the aid of electric generators, as well as in hydraulic pumps. The study of turbulent flow between rotating discs in Tesla turbines is extremely important to analyze the influence and the effects of rotation on the flow current lines, making it possible to foresee possible problems and allow the design to be changed without making the physical model for the experiment.

Given the need to seek alternatives for the electric power generation and the crescent scientific relevance been given for the study of MDT in this context, it is also necessary to study and evaluate the project of each component of an MDT. In this sense, this work aims to evaluate, through the numerical CFD method of a prototype tesla turbine built to evaluate the flow, pressure, and velocity profiles to confirm the theory about the model studied.

The tesla turbine has components that must be evaluated in detail, given their specific function of receiving the air coming from the compressor. Consequently, it produces torques with high velocity in the nozzle outlet, in order of sonic speed.

This type of equipment can operate with any work fluid available in gases lines of pneumatic systems. For the friction torque to occur satisfactorily, based on the spiral movement, the nozzle needs to receive the air along with a maximized speed, which will occur inside the nozzle, so that it provides a complete and continuous movement in a spiral form inside the turbine. To do so, the design and the configuration of the disc inside the turbine are fundamental

to study the improvement of the efficiency and to define the exact number of discs necessary to a determined torque. (Talluri, 2018).

The Figure 1 shows details for the Tesla turbine used in this work.

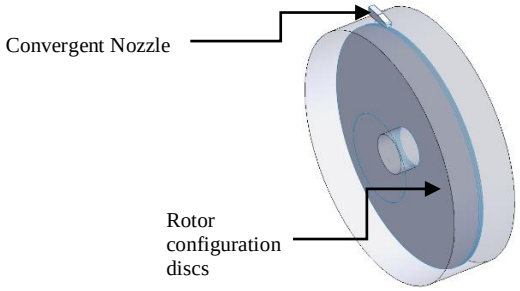

Figure 1. Details of Tesla turbine.

According to Çengel and Boles (2013), the fluid inlet temperature in the turbine is an important factor for performance evaluation. There are limitations to the temperature rising in a disorderly way since the components of the turbine need to be resistant to these temperatures. Therefore, evaluations of how a flow develops, its operation speed and temperatures during the cycle are extremely relevant.

2. Flow Simulation

The studied model was built in CAD 3D software, what can be observed in Figure 2 with an isometric and exploded view for understanding the parts of the assembly.

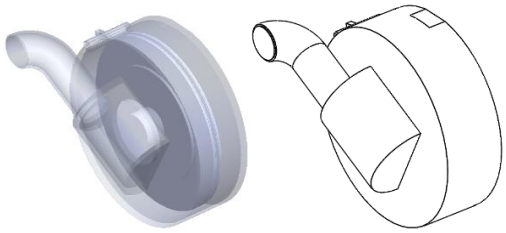

Figure 2. Tesla turbine CAD 3D. Isometric inside view (a) and outside contour (b) view.

The pressurized work fluid is admitted to the turbine and passes through a converging nozzle, which converts its pressure into sonic speed. The accelerated fluid passes through the rotor composed of parallel discs, describing a tangential path. The accelerated flow transfers its energy to the rotor through friction, which generates torque on the shaft. The fluid moves in a spiral form, remaining adhered to the walls of the discs until it reaches the discharge channels. These, in the form of a circular oblong, are positioned close to the central axis coupled to the discs, through which the fluid is discharged to the outside.

The torque generated by the friction of the fluid with the discs can be used in various applications, both for power generation with the aid of electric generators, as well as in hydraulic pumps.

For the study of the flow, the fluid was modeled as air and its properties in the input were defined by the physical experiments. The boundary conditions parameters applied in each geometry are defined according with the inlet pressure and mass flow, according to the Table 1.

Table 1. Air properties and parameters at the input boundary of the control volume considering the inlet temperature of 295.15 [K].

	Inlet gauge pressure [kPa]	Mass flow [kg.s-1]	Specific mass [kg.m-3]
Case 1	200	0.013	2.52
Case 2	250	0.018	2.91
Case 3	300	0.021	3.33
Case 4	350	0.025	3.75
Case 5	400	0.027	4.16

With standard air modeling, the fluid flow was modeled in a monophasic, compressible, and turbulent way, for the transient operating regime. To meet these conditions in numerical form, it is necessary to meet the resolution of a set of equations of mass, energy, and momentum conservation, as well as the Reynolds Number and Mach Number.

For characterization of the flow regime as laminar, transitory, and turbulent, the Reynolds number is used, as seen in Eq. (3), where V is the flow velocity, L is the characteristic length scale of the problem and μ, viscosity. According to Brunetti, 2008, in the case of tubes, the flow classification is: when Re < 2000, there is a laminar flow; when 2000 < Re < 2400, the flow is transient and Re > 2400 classifies a flow as turbulent, which presents vortices, among other instabilities in the flow.

$$Re = \frac{\rho V L}{\mu} \tag{3}$$

The flow of the working fluid through converging nozzles is limited to the sonic condition. Eq. (5) shows the mass flow rate per passage area in the nozzle throat $\dot{m}_t / A_t$, for an isentropic expansion and limited to the number of unit Mach.

$$\frac{\dot{m}_t}{A_t} = \frac{P_1}{\sqrt{T_1}} \sqrt{\frac{k}{R}} \left[\frac{1}{\left[\frac{k+1}{2}\right]^{\frac{k+1}{2(k-1)}}} \right] \tag{4}$$

2.1 Numerical methodology

An LBM commercial software was used in order to perform the CFD results calculated for the different turbine configurations. The XFlow software employs different turbulence models in its library, and it is still possible not to use any turbulence model to solve more complex simulation cases, however, the DNS turbulence modeling approach (Direct Numerical Simulation) for cases where the scales dissipative are greater than the resolution of the lattice grid (smallest resolved scale) a good simulation accuracy will be obtained with a higher computational cost. The simulations were carried out using the three-dimensional 3D kernel, single-phase, turbulent approach, using a Supersonic solver. To determine the turbulent flow properties, different turbulence models were considered according to the LES approach, described below.

The boundary conditions used were:

- Fluid properties calculated according with pressure and temperature conditions.
- Input condition: uniform pressure from 200 kPa to 400 kPa;
- Output condition: ambient pressure of 101.325 [kPa];

In this work, the Wall-Adapting Local Eddy (WALE) turbulence model is used to solve the flow, considering that this model has good properties both near and far from the wall and can be applied to both laminar and turbulent flows.

This model recovers the asymptotic behavior of the turbulent boundary layer when this layer can be resolved directly and does not add artificial turbulent viscosity in the off-tread shear regions. The WALE model is formulated as follows according to Eq. 5, using the Eqs. 6 to 9.

$$\nu_{turbulent} = \Delta^2 \frac{(G^d_{\alpha\beta} G^d_{\alpha\beta})^{\frac{3}{2}}}{(S_{\alpha\beta} S_{\alpha\beta})^{\frac{5}{2}} + (G^d_{\alpha\beta} G^d_{\alpha\beta})^{\frac{5}{4}}} \tag{5}$$

where:

$$S_{\alpha\beta} = \frac{1}{2}\left(\frac{\partial v_\alpha}{\partial r_\beta} + \frac{\partial v_\beta}{\partial r_\alpha}\right) \tag{6}$$

$$G^d_{\alpha\beta} = \frac{1}{2}\left(g^2_{\alpha\beta} + g^2_{\beta\alpha}\right) - \frac{1}{3}\delta_{\alpha\beta} g^2_{\gamma\gamma} \tag{7}$$

$$g_{\alpha\beta} = \frac{\partial v_\alpha}{\partial r_\beta} \tag{8}$$

$$\Delta = C_\omega Vol^{\frac{1}{3}} \tag{9}$$

where the WALE constant (C_ω) is typically 0.2.

In LES simulations, a turbulent vortex viscosity ν_t is added, is introduced to model the turbulence, and the turbulence viscosity is given in Eq. (10), by:

$$\nu_t = C^2{}_x \Delta x^2 \bar{\omega} \tag{10}$$

where C_x denotes the LES model dependent constant, Δx the grid spacing and $\bar{\omega}$ the operator of the LES model. In the lattice Boltzmann model, viscosity is related to relaxation time τ through Eq. (11).

$$\nu_{total} = \nu_0 + \nu_t = \frac{2\tau_0 - 1}{6} + \frac{\tau_t}{3} \tag{11}$$

where ν_0 is the molecular viscosity, analogous to the viscosity, the relaxation time τ is divided into two parts, one molecular and one turbulent.

The total relaxation time is defined in Eq. (12) as:

$$\tau_{total} = 3\nu_{total} + \frac{1}{2} \tag{12}$$

Applying Eq. (12) to Eq. (11), we arrive at Eq. (13).

$$\tau_{total} = 3(\nu_0 + (C_x^2 \Delta x^2)\bar{\omega}) + \frac{1}{2} \tag{13}$$

The total relaxation parameter τ_{total} is derived from the operator $\bar{\omega}$, which depends on the LES model and is a function of the shear stress tensor S and the rotation tensor Ω. The shear stress tensor S for Newtonian fluids is defined as Eq. (14):

$$S_{i,j} = \nu_0 \rho \left(\frac{\partial \pi_i}{\partial x_j} + \frac{\partial \pi_j}{\partial x_i} \right) \tag{14}$$

and the rotation tensor Ω for Newtonian fluids is given by Eq. (15):

$$\Omega_{i,j} = \nu_0 \rho \left(\frac{\partial \pi_i}{\partial x_j} - \frac{\partial \pi_j}{\partial x_i} \right) \tag{15}$$

For the calculation of the shear stress tensor S and the rotation tensor Ω, a central difference scheme can be applied, using the Boltzmann units of the network for the operator $\bar{\omega}$, and the scale $\Delta x = \Delta t = 1$, the parameter of turbulent relaxation τ_t is obtained in Eq. (16).

$$\tau_t = \frac{\sqrt{\tau_0^2 + \frac{18 C_x^2 \bar{\omega}^2}{\rho}} - \tau_0}{2} \tag{16}$$

The LES approach derived for the lattice Boltzmann scheme in its formulation has defined only the shear stress, considered as the tensor S, which corresponds to the Smagorinsky model.

The well-known fine structure model was found by Smagorinsky in 1963. He derived the operator $\bar{\omega}$ exclusively from the shear stress tensor as described in Eq. (17).

$$\bar{\omega} = \sum_{i,j} S_{i,j} S_{i,j} \tag{17}$$

Depending on the physical application, the constant of the LES model $C_X = C_S$ can to present values in the range of 0.05 and 0.16, according to the literature, this model is usually widely used for various industrial applications, from theoretical to experimental cases.

Hou, 1996, was the first to implement the Smagorinsky model in lattice Boltzmann. Krafczyk, et. al., 2003, applied it to the Boltzmann MRT 3D lattice scheme, however, with some limitations, some problems were evidenced due to the turbulent viscosity remaining positive even in laminar flows, while it is evident that ν_t is zero based on its definition, and yet, in other cases seen in the literature, in Smagorinsky's formulation, the law of the boundary layer of the wall is not respected.

According with Celik, 1999, in the Smagorinsky model, the turbulent viscosity ν_t is modeled by Eq. (18).

$$\nu_{turbulent} = \Delta^2|S| \tag{18}$$

where:

$$\Delta = C_s Vol^{\frac{1}{3}} \tag{19}$$

$$S = \sqrt{2S_{\alpha\beta}S_{\alpha\beta}} \tag{20}$$

where:

Δ is the filter scale, S is the strain rate tensor of the resolved scale and the Smagorinsky constant, C_s usually has a value between 0.1 and 0.2, recommended default value is $C_s = 0{,}12$.

A set of 27 PDFs on each lattice node, D3Q19 were used in theses simulations, each level resolves spatial (4th order) and temporal (2nd order) scales in twice as little time as the previous level, the Figure 3 presents this discretization scheme.

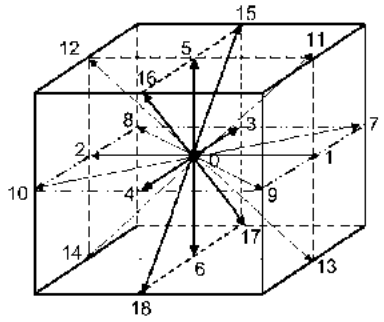

Figure 3. Lattice D3Q19 discretization.

The mesh generated with refinements in the regions near the walls, small spacings and regions of interest as flow areas between components, with five levels of refinements, and in the full domain has 6126558 elements, with the coarsest resolved length in 0.012 m, with the Prandtl number of 0.741114.

Table 2 shows the different lattice parameters used to determine the inherent error of the mesh resolution in the CFD study, was calculated through the comparison of results calculated for three different sizes of the lattice grid.

Table 2. Lattice properties and voxel size parameters

Mesh	Voxels	Minimum element size (mm)	Maximum element size (mm)
refined	7789330	0.01375	3
intermediate 2	6126158	0.750	12
intermediate	2756771	1.00	20
coarse	1926800	1.20	30

The main three different voxels configurations generated with refinements in the regions near the walls and calculated with the Courant number of 1. The refinement parameter for the dimensional control of the lattices of the regions close to the wall was the refinement of near static walls, for the representation with a finer resolution than the scale to be resolved close to the geometries, as illustrated in Figure 4, where the voxels are presented in a plane slightly close to the walls of the disc surfaces.

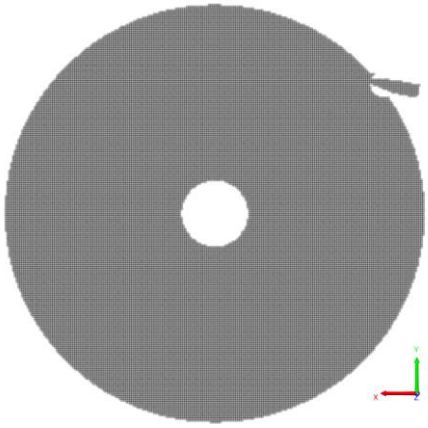

Figure 4. Voxels adjacent to disc surfaces with the algorithm for handling smaller voxels near walls.

Figures 5 and 6 illustrate the voxels generated in the internal regions of the turbine with the turbine disc configuration 2 a, it is noted that it is predominantly composed of smaller voxels where the wall of some component is the limiting factor of the beginning and end of the lattice structure, in the region between the discs the refining is evident and visibly greater in relation to the regions away from the wall.

The pattern of increase in the size of the voxels with regions of refinement performed through the definition of the used algorithm defined previously in the text is also visualized.

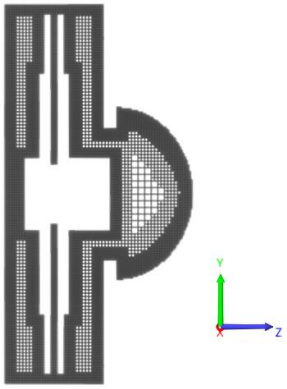

Figure 5. Voxels generated on a surface orthogonal to the axis of the Tesla turbine with reduced voxel size close to the walls – Turbine 2 disc configuration

The Figure 6 illustrates, in an analogous way to the previous figure, the same behavior of the definition of the voxels with the lattices varying in size along the internal domain of the turbine.

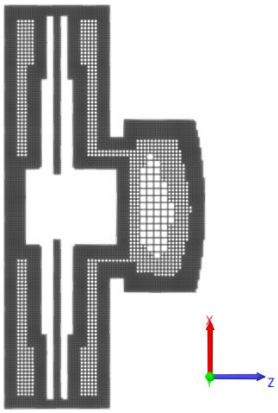

Figure 6. Voxels generated on a surface orthogonal to the Tesla turbine axis with reduced voxel size close to the walls

It should be noted that the same mesh parameters were adopted for the evaluation of the different turbine configurations analyzed in this work, considering that in the preliminary studies, no significant variation was verified in the results calculated by the code, in addition to the similarity between the values for the parameters analyzed in the simulations, of torque, speed, Mach number, as well as the behavior of the internal flow in the internal regions of the turbine.

2.2 Results

This chapter presents the main numerical studies carried out with the code used for the fluid dynamics analysis of the Tesla turbine analyzed, a description of the cases that were solved computationally, as well as the boundary conditions applied to the different simulated conditions.

Results of a self-verification study performing the parametric variation of the ends of the turbine discs are also presented, where different operating conditions were used to evaluate the behavior of the numerical model proposed to solve the flow in the Tesla turbine in question.

Given the operating conditions, pressure and flow, and specific mass of the working fluid, and the torque result from the numerical calculations obtained with the computational code elaborated in this work, the Torque column being measured from a result obtained experimentally through physical tests on the bench with their respective percentages of uncertainty. Finally, the percentage variation between the numerical torque results in relation to the measured torque is summarized in the last column of each table.

The configurations varying quantity and discs spacing are show in the Figure 7.

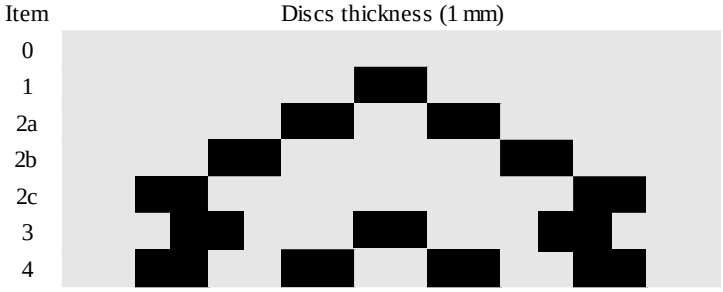

Figure 7. Tesla turbine discs configurations varying quantity and discs spacing

Table 3 refers to the Tesla turbine configuration with zero discs and presents the measured torque results referring to the bench-top results with the turbine prototype tested in the laboratory with its associated measurement uncertainty of 3.45%, and the results of the numerical study called torque CFD, and the percentage variation between the values measured experimentally with the values obtained numerically, using the experimental result as a reference.

Table 3. CFD calculations data for the Tesla turbine design using 0 Discs configuration.

Inlet gauge pressure [kPa]	Mass flow [kg.s-1]	Specific mass [kg.m-3]	Torque CFD [N.m]	Torque [N.m]	% Torque CFD X Torque
200	0.013	2.52	-	-	
250	0.018	2.91	0.38	0.42	9.52
300	0.021	3.33	0.51	0.53	3.77
350	0.025	3.75	0.63	0.67	5.97
400	0.027	4.16	0.82	0.79	3.79

Graphically in the next figures, we have the experimental results and those calculated via computational fluid dynamics for the different configurations of the Tesla turbine, which are summarized in the figures below, associating the uncertainty range for the experimental results, in order to enable the comparative analysis of the calculated results. for the simulated torque that are close to the range of uncertainty associated with the experimental data, starting in Figure 8 with zero discs configuration.

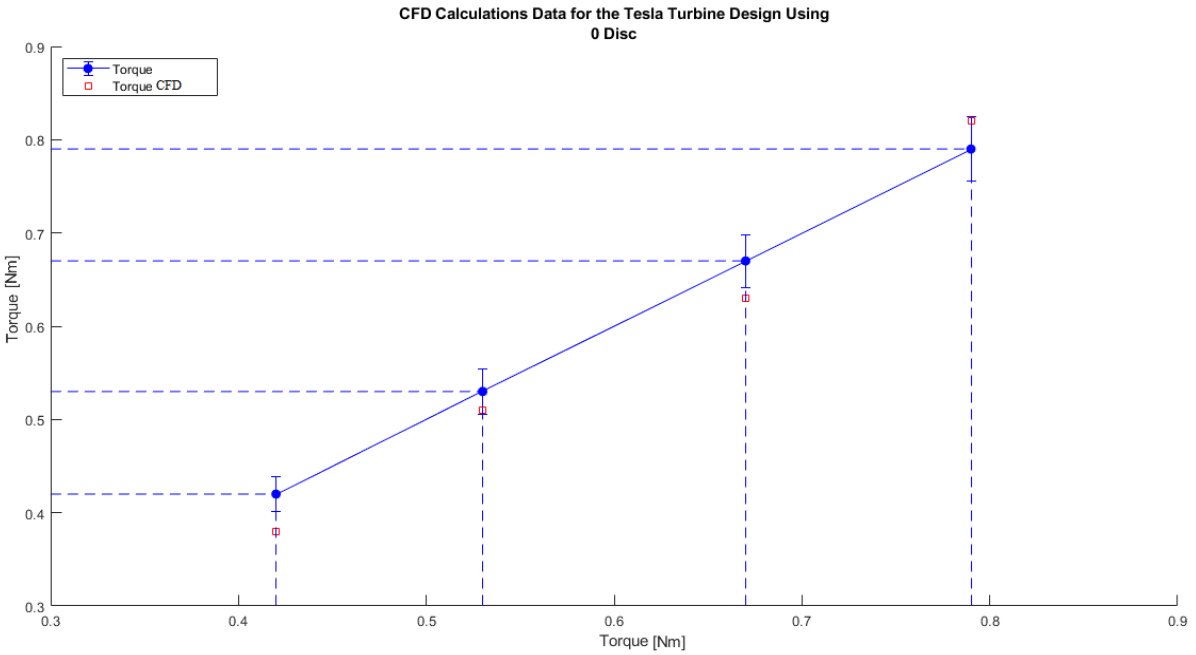

Figure 8. Graph with the measurement uncertainty of the measured torque with the calculated torque result (CFD) for the Tesla turbine configuration 0 discs

The next numerical results calculated for the design configuration using 1 to 4 disc configurations are presented in Table 4 through Table 9, where the spacings between the discs vary from the center of the rotor, and from the end of the rotor, both with spacing of 1 mm.

Table 4. CFD calculations data for the Tesla turbine design using one disc.

Inlet gauge pressure [kPa]	Mass flow [kg.s-1]	Specific mass [kg.m-3]	Torque CFD [N.m]	Torque [N.m]	% Torque CFD X Torque
200	0.013	2.52	0.45	0.41	9.7
250	0.018	2.91	0.62	0.59	5.08
300	0.021	3.33	0.83	0.78	6.41
350	0.025	3.75	1.02	0.95	7.36
400	0.027	4.16	1.18	1.13	4.4

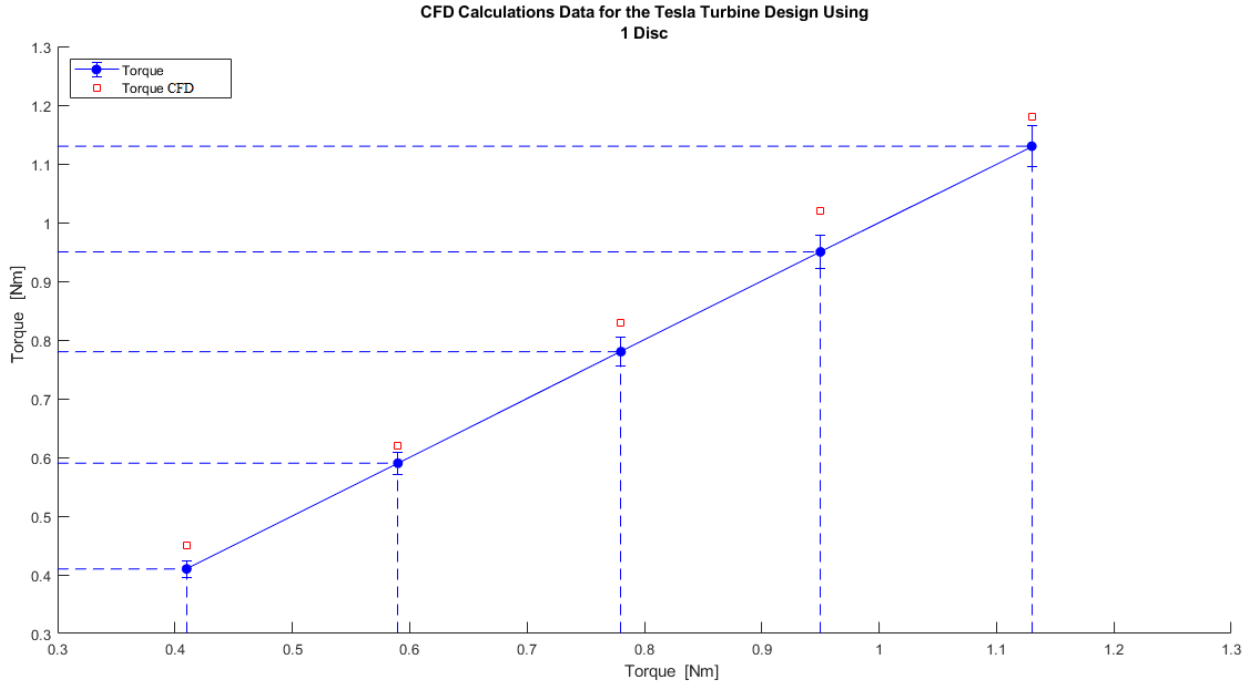

Figure 9. Graph with the measurement uncertainty of the measured torque with the calculated torque result (CFD) for the Tesla turbine configuration 1 disc

Table 5. CFD calculations data for the Tesla turbine design using 2a discs.

Inlet gauge pressure [kPa]	Mass flow [kg.s-1]	Specific mass [kg.m-3]	Torque CFD [N.m]	Torque [N.m]	% Torque CFD X Torque
200	0.013	2.52	0.34	0.35	2.85
250	0.018	2.91	0.51	0.54	5.55
300	0.021	3.33	0.63	0.70	10
350	0.025	3.75	0.79	0.90	12.22
400	0.027	4.16	0.98	1.06	7.54

Table 6. CFD calculations data for the Tesla turbine design using 2b discs.

Inlet gauge pressure [kPa]	Mass flow [kg.s-1]	Specific mass [kg.m-3]	Torque CFD [N.m]	Torque [N.m]	% Torque CFD X Torque
200	0.013	2.52	0.36	0.40	10
250	0.018	2.91	0.55	0.60	8.33
300	0.021	3.33	0.72	0.78	7.69
350	0.025	3.75	0.92	0.97	5.15
400	0.027	4.16	1.32	1.14	15.78

Table 7. CFD calculations data for the Tesla turbine design using 2c discs.

Inlet gauge pressure [kPa]	Mass flow [kg.s-1]	Specific mass [kg.m-3]	Torque CFD [N.m]	Torque [N.m]	% Torque CFD X Torque
200	0.013	2.52	0.36	0.35	2.85
250	0.018	2.91	0.62	0.57	8.77
300	0.021	3.33	0.85	0.75	13.33
350	0.025	3.75	0.95	0.98	3.06
400	0.027	4.16	1.09	1.16	6.03

Table 8. CFD calculations data for the Tesla turbine design using 3 disc.

Inlet gauge pressure [kPa]	Mass flow [kg.s-1]	Specific mass [kg.m-3]	Torque CFD [N.m]	Torque [N.m]	% Torque CFD X Torque
200	0.013	2.52	0.38	0.36	5.55
250	0.018	2.91	0.55	0.58	5.17
300	0.021	3.33	0.79	0.78	1.28
350	0.025	3.75	0.95	1.00	5
400	0.027	4.16	1.17	1.22	4.1

Table 9. CFD calculations data for the Tesla turbine design using 4 disc.

Inlet gauge pressure [kPa]	Mass flow [kg.s-1]	Specific mass [kg.m-3]	Torque CFD [N.m]	Torque [N.m]	% Torque CFD X Torque
200	0.013	2.52	0.52	0.48	8,33
250	0.018	2.91	0.71	0.68	4,41
300	0.021	3.33	0.82	0.87	5.74
350	0.025	3.75	0.98	1.03	4,85
400	0.027	4.16	1.19	1.21	1.66

3. CONCLUSIONS

With the study carried out for the different disc topologies, it is evident that the turbine maintains a linear behavior pattern for the Torque results, and consequently, the energy generated by the turbine can be better dimensioned with the geometric variations presented here for the correct operating pressure ranges, shown here between 350 kPa and 400 kPa. It is observed that the percentage variation between the torque results presented, presenting mostly results with the associated measurement uncertainty below 10%, with a minimum average value of 0.51% and a maximum average variation of 5.94%.

Preliminary studies made it possible to understand the behavior of the code, as well as its sensitivity to changes in the boundary conditions used. Considering the measurement uncertainty associated with 3.45% of the measured torque values, the vast majority of the results presented here contain values within the uncertainty range, a percentage of 8.82% of the numerically calculated results were obtained above of 10% of variation in relation to the experimental results, and about more than 91.18% of the results calculated with the CFD numerical code used in this thesis were below 10% of variation of the results measured on the bench using a physical prototype of the Tesla turbine studied.

4. REFERENCES

BATISTA, J. C. Microgeração de energia elétrica (abaixo de 100 kw) utilizando turbina tesla modificada / Júlio César batista. Guaratinguetá: [s.n], 2009.

BRUNETTI, F. Mecânica dos fluidos. 2 ed. São Paulo: Pearson Prentice Hall, 2008.

Çengel, Y. A., Boles, M.A., 2013, Termodinâmica. Porto Alegre: Amgh.

CELIK, I. B. Introductory Turbulence Modeling. West Virginia University Mechanical & Aerospace Engineering Dept. Morgantown, 1999.

HOU, et al. A lattice Boltzmann subgrid model for high Reynolds number flows. Fields Institute Communications 6 (1996) 151–165.

KRAFCZYK, M. J. Tölke, L.S. Luo. LES simulations based on a multiple relaxation time LB model. International Journal of Modern Physics B 17 (2003) 33–39.

KARTHIK, T. S. D. Turbulence models and their applications. Department of Mechanical Engineering IIT Madras: 10th Indo German Winter Academy, 2011.

5. RESPONSIBILITY NOTICE

The authors are the only responsible for the printed material included in this paper.